



## EVALUATION OF SEISMIC BEHAVIOR FOR MOMENT FRAMES AND ECCENTRICALLY BRACED FRAMES DUE TO NEAR-FIELD GROUND MOTIONS

L. Haj Najafi\*<sup>1</sup> and M. Tehranizadeh<sup>2</sup>  
Department of Civil and Environmental Engineering, Amirkabir University of  
Technology, Hafez Avenue, Tehran, Iran.

**Received:** 5 June 2012; **Accepted:** 30 September 2012

### ABSTRACT

This research aims to evaluate seismic behavior of moment frames (MF) and eccentrically braced frames (EBF), two common systems in most of the steel codes, due to far-field and near-field ground motions and to propose practical technique for acquiring demand distributions. Much intensive amounts and distinct patterns of demand are recognized according to near-field records. Also, the results demonstrate distinctive dissimilarities in demand distributions, their rate of changes and intensities and different higher mode participation patterns in MF and EBF systems. In addition, calculated R factors and these parameters in ASCE and UBC codes were compared thoroughly in this study.

**Keywords:** Near-field; far-field; moment Frame (MF); eccentrically braced frame (EBF); nonlinear time history analysis; pushover analysis.

### 1. INTRODUCTION

#### *1.1. Introduction to Near-field Records*

After Loma Prieta 1989 earthquake, Mohraz has divided earthquakes into three groups:

- Near-field earthquakes: the distance between site and fault is less than 20 km,
- Mid-field earthquakes: the distance between site and fault is between 20 km to 50 km,
- Far-field earthquakes: the distance between site and fault is more than 50 km [1].

This classification according to distance is not exactly precise and in some research studies the distance of near-field records is considered less than 10 or 15 km. [2]. Near-field earthquakes have some distinct characteristics in comparison to far-field ones like higher amounts of acceleration and restricted frequency content in high frequencies. Also, their records have some pulses in the beginning of their accelograms with high periods and large

---

\* E-mail address of the corresponding author: lila\_najafi@aut.ac.ir (L. Haj Najafi)

amounts of domain that are much considerable in the situation of forward directivity contributing to record transmission from board-band condition to pulse-like ones. These pluses bring about occurrence of maximum amount of Fourier spectrum in limited periods unlike the maximum of Fourier spectrum in far-field records that occurs in wide-range of periods [3, 4]. These pulses also cause the domination of wave-like terms on mode-like ones for demand distribution in height of buildings mostly affecting structural responses. [4]. Transmitting maximum value of domain to the smaller periods along with intensifying virtual stiffness and reducing structural damping ratio are the other effects of propagation of record pulses in height of buildings [5].

The ratio of vertical to horizontal spectrum in near-field records is much greater than far-field ones. This ratio is often considered as 0.667 in most of the codes. But, in near-field earthquakes this ratio can reach to number 2 in short periods [5].

The above explanation shows lots of differences between near-field and the other earthquakes contributing disparate structural responses under these records. Differences between bam (near-field) and Morgan (far-field) records could be seen in Fig. 1.

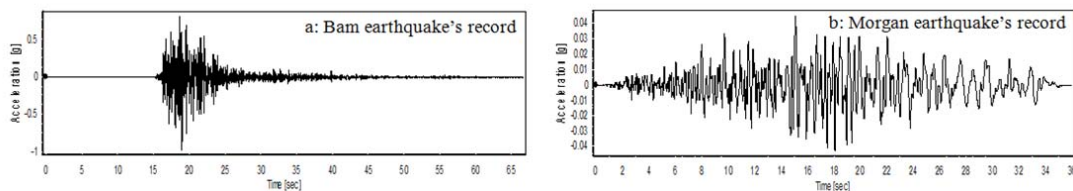


Fig. 1. Comparing the differences between a: bam (near-field) and b: Morgan (far-field) earthquakes.

## 1.2. Introduction to Structural Systems

### 1.2.1. Moment resisting frames (MF)

Moment resisting frame generally consists of rectangular subdivisions with horizontal beams and vertical columns. This system has appropriate ductility in comparison with the other structural systems, however because of low stiffness, lateral displacement limitations are hardly satisfied especially for tall buildings; thus, application of MF for tall building designs will be non-economical.

The nonlinear deformations in MFs take place in particular points which could modify to hinge and suffer large rotations with almost constant forces in large inelastic strains. Hinges often occur in the ends of a beam at beam-column connections or in the place of occurring maximum moment between two ends of a beam. An expert designer should avoid hinge fabrication in columns. Northridge earthquake taught designers to get distance between hinge occurrence points and the connection sections between beams and columns. All details about steel moment frame design are available in most of the steel codes. One general moment frame and arbitrary hinge locations causing instability in the frame were shown in Fig. 2 (a).

### 1.2.2. Eccentrically braced frames (EBF)

In eccentrically braced frames, lateral behavior of structure is the combination of axial forces, shears and moments of the beams and columns and the compressions and tensions of

braces in the braced spans. In these systems braces in each span are located with distance in longitudinal axis of beam or with distance by beam to column connections.

These systems are expected to withstand significant inelastic deformations in the links whereas other segments of the system (out of link-beam) shall be designed to remain essentially elastic; therefore, although having convinced ductility, it has sufficient stiffness too. The EBF's ductility and stiffness change by changing the length of link-beam and therefore can be set to get optimum condition. The aim of designer is not preventing hinge production; however, the object is controlling hinge development positions, and providing adequate rotation capacity for link-beams [6]. Samples of eccentrically braced frames could be seen in Fig. 2 (b).

The length of link-beams affects the type of hinges and consequently the type of mechanism. Considering the stability equation, these two boundaries were gained for link-beams.

$$e \leq \frac{1.6M_p}{V_p} \quad \text{Shear Link-beams,} \quad (1)$$

$$e > \frac{2.6M_p}{V_p} \quad \text{Moment Link-beams.} \quad (2)$$

Where  $e$  is the length of link-beam,  $M_p$  is the amount of plastic moman and  $V_p$  is the amount of plastic shear. When the length of link-beam is between these limitations both shear and moment mechanisms occur simultaneously.

UBC code confines the ultimate rotation of link-beams,  $\theta = 0.09$  for shear-links and  $\theta = 0.03$  for moment-links; however, AISC limitations are  $\theta = 0.08$  for shear-links and  $\theta = 0.03$  for moment-links and these limitations in Iran's code are  $\theta = 0.08$  for shear-links and  $\theta = 0.02$  for moment-links.

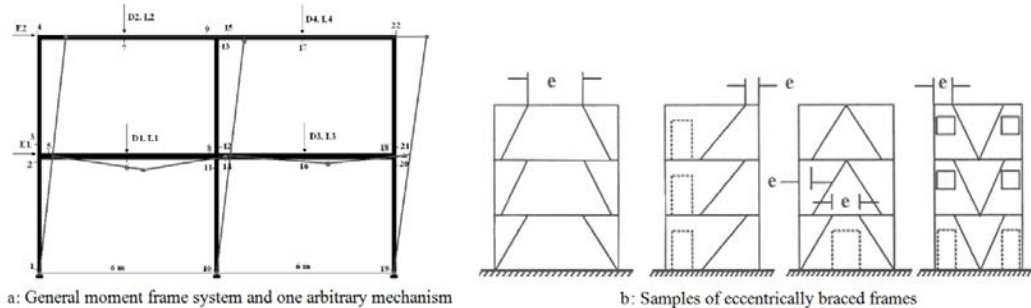


Fig. 2. General samples of moment frame and eccentrically braced frame systems

## 2. RECORDS

All employed near-field records in this research have source-to-site distances less than 10 km and all of them except the Bam and Chichi records are picked up from [7], [8]. The Bam and Chichi records were derived from the websites of [9] and [10] respectively. All

incorporated records were registered in soil type D based on NEHRP, equal to Zone 4 of UBC [6] and soil class II according to Iran Seismic Code (2800) [11] or adjusted for this type of soil. All of the record's stations have distance less than 10 km and for all of them  $6.2 \leq M_w \leq 7.4$ , as shown in Table 1. Three far-field records were applied to comprehend the comparison with distances above 50 km and not containing any pulse-like waves presented in Table 2 [8].

### 3. MODELING AND DESIGN

In this research, the moment frames with two ductility levels, Intermediate and special ductility, and eccentrically braced frames with short and long link-beams have been modeled having residential occupancy. The lengths of link-beams were respectively considered equal to 0.5 m and 3.0 m for short and long link-beams. Buildings were modeled with three, five, eight and fifteen number of stories and the height of each story is considered equal to 3 m. Loading and complete design of each model is individually done incorporating very high earthquake probabilistic hazard level according to Iran Seismic Code (2800) [11], much similar to UBC97 [6], and Iran's Steel Design Code [12], much similar to AISC2005 [13] by the means of Sap2000 software that is a very common software for analyzing and design of structures. All the stories have similar and regular plans with four longitudinal spans and three spans in the other side that each span was equal to 4 m and the accidental torsion was considered equal to 5% . Considered plan and position of braces could be seen in Fig. 3.

IPE, BOX and UNP double sections are correspondingly used for beams, columns and braces and all of them are chosen to be compact. Sections in different stories were chosen by considering regularity in hinge production in height; it means that before producing plastic hinges in all of the stories, the structure does not go under instability and collapse mode.

Definition of plastic hinges and nonlinear static analysis were executed based on FEMA273 [14], considering P- $\Delta$  effects in all analyses. In addition, all the linear dynamic analyses were done as modal transient time history analyses applying Eigenvector method and all the nonlinear dynamic analyses were performed as direct integration transient time history analysis using direct integration in Hilber, Hughes and Taylor's (HHT) method by considering damping ratio for all modes equal to 5%.

Table 1: Specification of near-field ground motions

Earthquake	Year	Station	Distance (km)	$M_w$	Duration (sec)
Tabas	1978	Tabas	1.2	7.4	32.840
Bam	2003	Bam	1	6.8	66.555
<i>Loma Prieta</i>	1989	Los Gatos	3.5	7	24.96
<i>Mendocino</i>	1992	Petrolia	8.5	7.1	35.98
<i>Erzincan</i>	1992	Erzincan	2	6.7	20.775
<i>Landerz</i>	1992	Lucerne	1.1	7.3	48.12
<i>Northridge</i>	1994	Olive View	6.4	6.7	39.98
<i>Kobe</i>	1995	JMA	0.6	6.9	47.98
<i>Chichi</i>	1999	TCU068	1.09	7.6	90.00

Table 2: Specification of far-field ground motions

Earthquake	Year	Station	Distance (km)	$M_w$	Duration (sec)
Tabas	1978	Ferdoos	94.4	7.4	40.00
Morgan Hill	1984	Morgan	76.25	6.8	35.995
Landerz	1992	12026 Indio	55.7	7.3	60.00

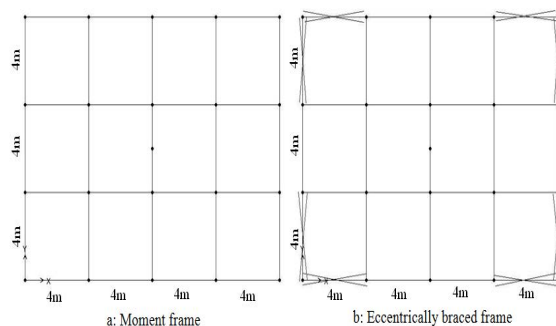


Fig. 3. Plan of each story for a: Moment frame and b: Eccentrically braced frame systems.

#### 4. EVALUATION OF RESULTS

As there are several systems with different properties subjected to various records, we should choose a method for evaluating and comparing the results in an easy and understandable manner. Referring to Fig. 4, there are several patterns of story shear distribution subjected to near-field and far-field records. It is obvious that for evaluation of results, it is not possible to compare the diagrams one by one and a straightforward method should be substituted.

Utilizing mean value is the one way of assessing the result easily. The error of this simplification is assessed through calculation of standard deviations which are presented in Fig. 5 and Fig. 6 for different number of stories, different analysis methods and for two groups of records for SMF and EBF systems and it is discovered that dissimilarities between standard deviations of nonlinear analysis under near-field earthquakes and these parameters from linear analysis or under far-field ones, are extremely large.

In favor of better understanding about the dispersion of results around the mean value, the dispersion ratio ( $\beta$ ) was calculated by equation (3).

$$\beta = \frac{\sigma}{\mu} \quad (3)$$

Where:  $\beta$ : Dispersion ratio,  $\sigma$ : Standard deviation and  $\mu$ : Mean value.

Values of  $\beta$  for SMF and EBF systems with short link-beam (length of link-beam:  $e = 0.5$  m), are got in Table 3. It could be seen that there is less dispersion for EBF systems than MF systems demonstrating more accuracy in application of mean values for EBFs than MFs. In addition, the evaluations have showed that for both systems the amounts of standard deviation gained from nonlinear dynamic analysis are remarkably high and the mean values

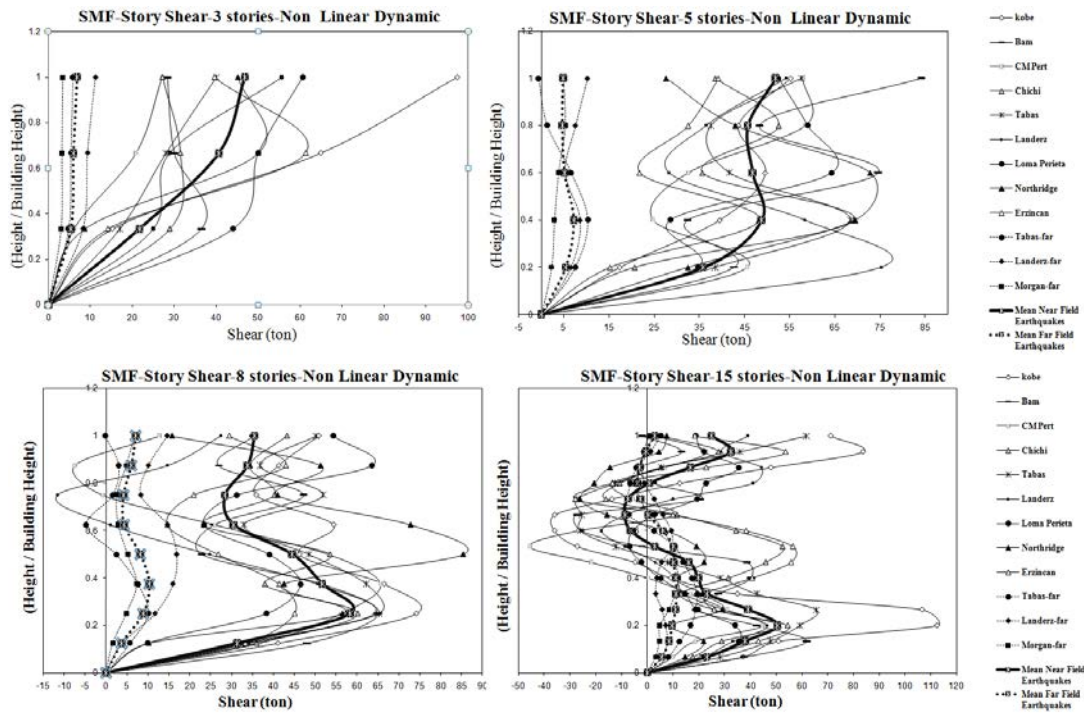


Fig. 4. Story shear for SMF systems by different number of stories for each record and the distribution of the mean values for near- and far-field records from nonlinear dynamic analysis

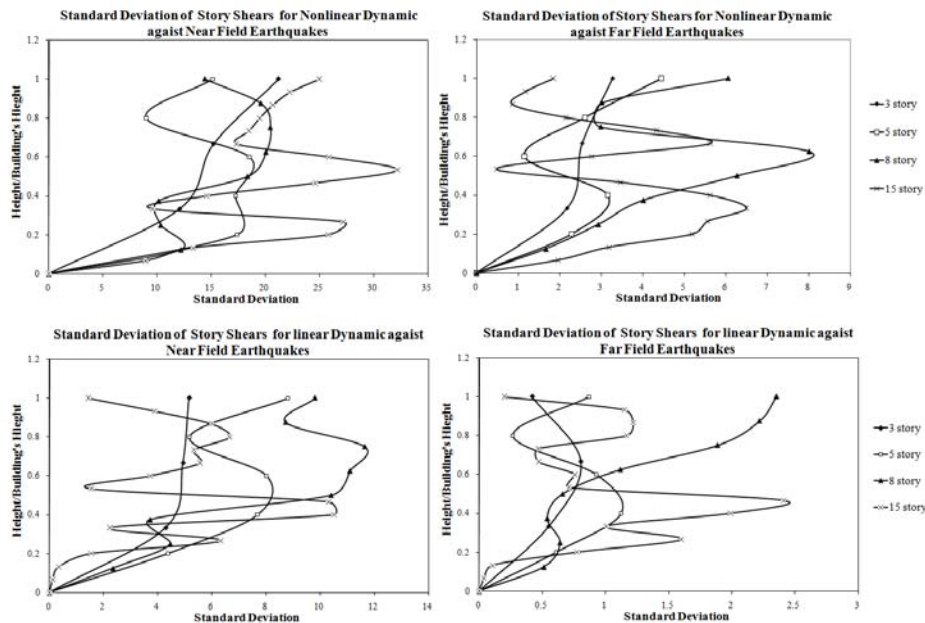


Fig. 5. Standard deviations of story shears under near-field and far-field records for SMF systems

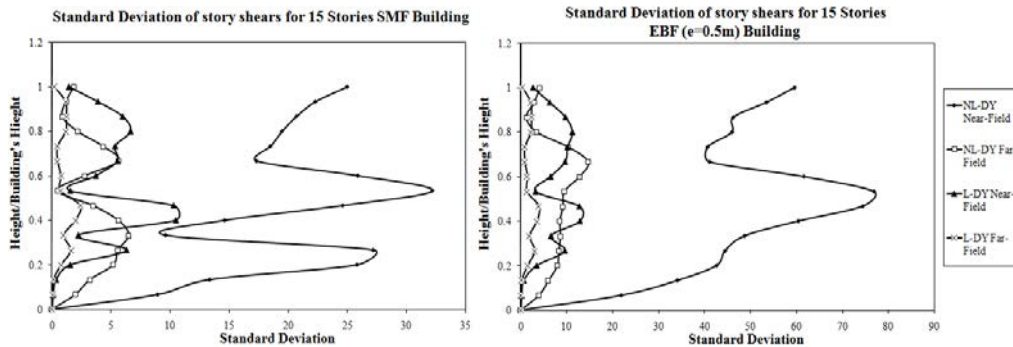


Fig. 6. Standard deviations of story shears for SMF and EBF systems with 15 stories against near and far-field records under linear and non linear dynamic analysis

Table 3:  $\beta$  for story shears from nonlinear dynamic analysis under near-field records for SMF and EBF systems

Systems	No of Story															
		1	2	3	4	5	6	7	8	9	10	11	12	13	14	15
SMF Systems	3 Story SMF Building	0.56	0.37	0.45												
	5 Story SMF Building	0.48	0.35	0.40	0.20	0.29										
	8 Story SMF Building	0.39	0.18	0.20	0.41	0.66	0.72	0.58	0.41							
	15 Story SMF Building	0.39	0.35	0.51	0.69	0.42	0.74	1.53	11.14	4.04	2.01	2.48	22.26	1.24	0.69	1.00
EBF (e=0.5m) Systems	3 Story SMF Building	0.30	0.31	0.33												
	5 Story SMF Building	0.39	0.21	0.10	0.09	0.16										
	8 Story SMF Building	0.25	0.22	0.25	0.30	0.41	0.37	0.45	0.39							
	15 Story SMF Building	0.35	0.34	0.34	0.31	0.32	0.40	0.54	0.61	0.58	0.49	0.66	0.97	1.00	0.94	0.94

4.1. Evaluation of Lateral Forces

4.1.1. Evaluation of lateral forces under nonlinear analysis

It has been shown in Fig. 7 that the least lateral story shears are in SMF systems and the most are in EBF systems with short link-beams from nonlinear dynamic analysis. Also, it could be recognized that for far-field records, lateral story shears for different systems are very close to each other, but in near-field ones considerable dissimilarities are perceived.

Because of more shear in EBF systems with short link-beams, the negative or inverse story shears have not been observed in their diagrams, whereas for the other systems negative shears usually exist in some stories below the roof story. As columns are usually designed for positive moments and not for inverse ones, these negative shears influence design procedure of the columns in these stories.

It could be seen for all systems under both near and far-field earthquakes by raising the number of stories, the maximum story shear moves to the lower height ratios. This fact is intensely observed in SMFs than the other systems. For instance, in a 3-story SMF model under near-field records the maximum story shear occurred in story 3 (height ratio=1), in 5-story SMF model occurred in story 3 (height ratio=0.6), in 8-story SMF model occurred in story 2 (height ratio=0.25) and in 15-story SMF model occurred in story 3 (height ratio=0.2). Whereas, for EBF systems with long link-beams under near-field records the maximum story shear for 3-story model occurred in story 3 (height ratio=1), 5-story model occurred in story 3 (height ratio=0.6), 8-story model occurred in story 3 (height ratio=0.375) and 15-story model occurred in story 5 (height ratio=0.33).

4.1.2. Evaluation of Modal Participations

As it could be anticipated before, the modal participation increases by increasing the height of building shown in Fig. 8.

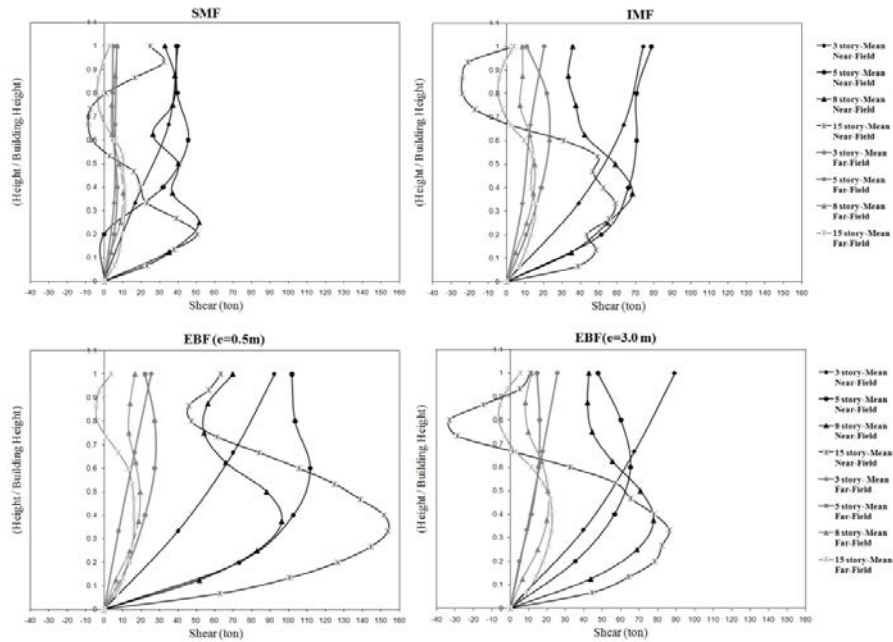


Fig.7. Lateral force distributions under near field and far field records from nonlinear dynamic analysis

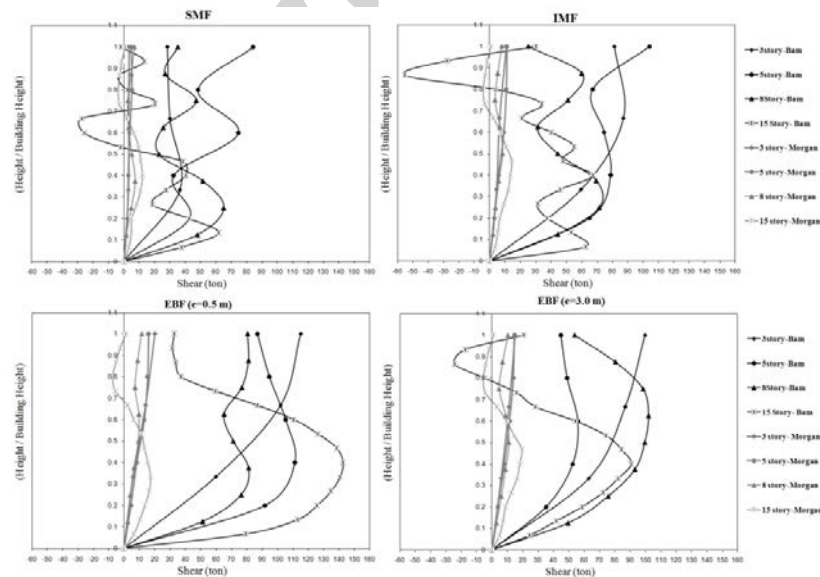


Fig.8. Modal participation under near-field and far-field records from nonlinear dynamic analysis



If we notice Fig. 8 more cautiously, it will be detected that the mode participation for Bam (near-field) record is much more than Morgan (far-field) one. This is because of the wave-like characteristic of this type of records that was mentioned previously in section1. This characteristic cause the wave of earthquake record, especially the record's vertical component propagates in height of structure. Also, containing more intense vertical records, amplification of mode participation occurred in the results under near-field earthquakes more than far-field ones. Mode participation could be noticed in moment frame systems much more than EBF systems and it is one of the important motivations for transmission of maximum story shear to lower height ratios and occurrence of negative shears.

4.1.3. Evaluation of lateral forces under linear dynamic and static analysis

Lateral force distributions in various systems by different number of stories under near-field and far-field records from linear dynamic and linear static analysis were displayed in Fig. 9. It could be inferred that for all of the systems, the results from far-field records are less than linear static results and the results from near-field records are approximately equal or more than linear static results particularly in the middle stories. Similarities between the results from linear dynamic analysis under near-field earthquakes with the linear static results in MF systems are more than EBF systems. It could be concluded that utilizing linear static results for design is satisfying if the seismic hazard of the site is controlled only by far-field records. However, in the regions with high occurrence probability of near-field earthquakes, using linear static method could cause inadequacy in lateral shear capacity especially in the middle stories of EBF systems.

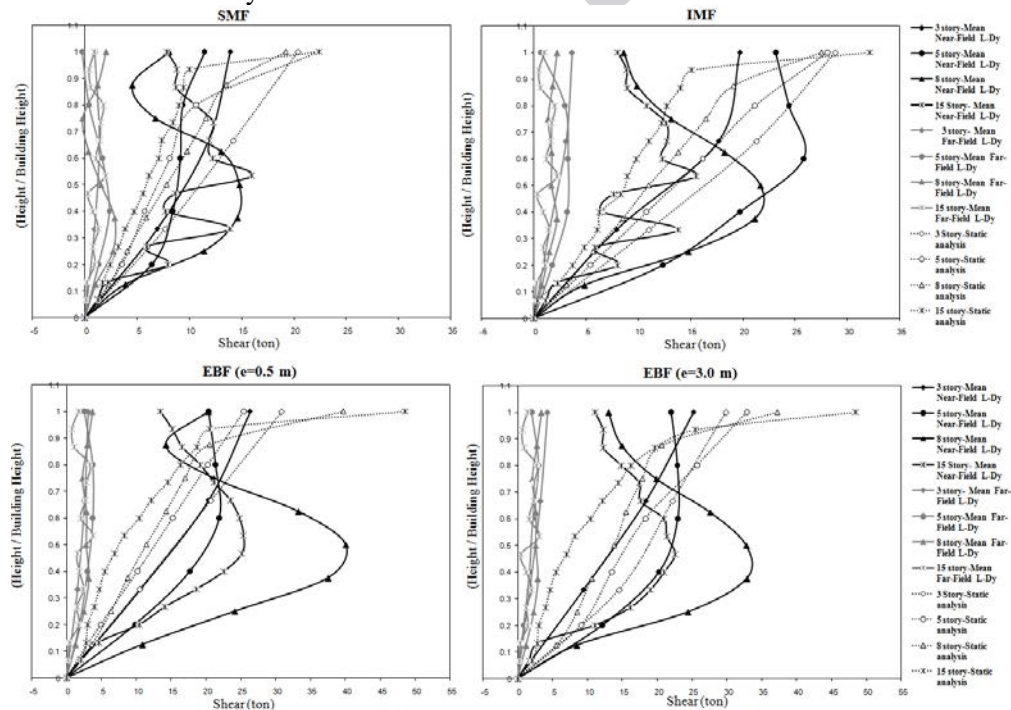


Fig.9. Lateral force distributions under near and far-field records from linear dynamic and static analysis

Similar to the results gained from nonlinear dynamic analysis, the least lateral story shears are in SMFs and the most are in EBFs with short link-beams from linear dynamic analysis and mode participation are more in MF than EBF systems. Going back to Fig. 7, it could be observed that the EBFs with short link-beams are able to suffer more lateral forces than EBFs with long link-beams in nonlinear analysis, but in linear analysis the distributions and amounts of lateral forces in both systems are close to each other showing that the nonlinear capacity of EBFs with long link-beams is less than this system with short link-beams as well as the most portion of shear carrying capacity of EBFs with short link-beams is in nonlinear region.

#### 4.2. Evaluation of Lateral Displacements

It has been shown in Fig. 10 that the most lateral displacements are in SMFs and the least are in EBFs with short link-beams from nonlinear dynamic analysis as well as mode participation effects are seen more in SMF's lateral displacement in comparison with the other systems. Also, it could be observed that lateral displacements for different systems are very close to each other under far-field records.

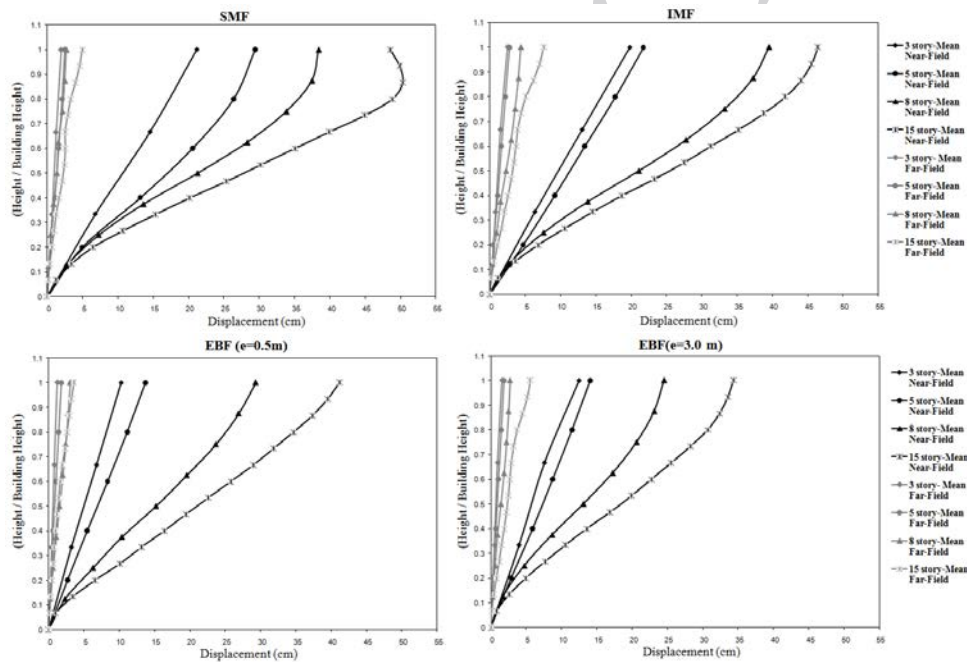


Fig.10. Lateral displacement distributions under near and far field records from nonlinear dynamic analysis

It could be inferred from nonlinear dynamic analysis that in EBF ( $e=3.0\text{m}$ ) with 3 and 5 stories lateral displacements are more than EBF ( $e=0.5\text{m}$ ). But by rising the number of stories and extending the nonlinear behavior of the models, lateral displacements in EBF ( $e=0.5\text{m}$ ) become more than EBF ( $e=3.0\text{m}$ ). The reason is that the EBFs with short link-beams have more ductility and could go in nonlinear region more than EBFs with long link-beams. In addition, considering Fig. 7 and Fig. 10, we could deduce that EBFs with short

link-beams could suffer more story shear as well as more lateral displacement than the EBFs with long link-beams. If we consider the fact of greater linear dynamic displacements in EBF ( $e=3.0\text{m}$ ) than EBF ( $e=0.5\text{m}$ ) in all of the models, the majority of nonlinear portion of lateral displacement in EBFs with short link-beams could be figured out. Furthermore, since ductility could be defined as maximum nonlinear displacement divided by maximum elastic displacement, containing more ductility by EBFs with short link-beams in comparison to EBFs with long link-beams could be anticipated.

#### 4.3. Evaluation of Nonlinear Parameters

According to FEMA273 [14], two distributions were applied for lateral forces. First, uniform lateral distribution and second, corresponding to shear values from linear spectrum analysis. Two gravitational load combinations were used too,  $Q_G = 0.9Q_D$  and  $Q_G = 1.1(Q_D + Q_L)$ . We adjoin to these distributions, the lateral distribution according to story shear patterns from linear static in company with the gravitational load of  $Q_G = Q_D + Q_L$ . Furthermore, there are accidental torsions in each direction equal to  $\pm 5\%$  and considering two directions for each lateral load, as there are 16 models, 320 nonlinear static analyses should be done.

$$16(\text{models}) \times 2(\text{torsion}) \times 2(\text{directions}) \times (2 \times 2 + 1) (\text{gravitational} + \text{lateral loads}) = 320$$

Among 20 nonlinear static analyses for each model, critical analysis with the least maximum nonlinear displacement has been chosen for investigation. The pushover diagrams have been shown in Fig. 11. Some common parameters are often used for assessing the behavior of structures in nonlinear zone that could be described as:

T: Period of the model

W: Weight of model, defined as  $Q_D + \alpha Q_L$ , where  $\alpha$  gotten from [11]. (here  $\alpha=0.2$ )

$F_{\max}$ : Maximum base shear suffered by the model before collapse.

$F_y$ : Yield base shear, model's shear when yielding starts that was determined in accordance to FEMA273 [14] guidelines.

$\Delta_{\max}$ : Maximum displacement occurred in the control point of whole structure. (Control point is usually recognized as the stiffness center in the roof level)

$\Delta_y$ : Yield displacement corresponding to  $F_y$

$$\mu: \text{Ductility factor, } \mu = \frac{\Delta_{\max}}{\Delta_y} \quad (4)$$

$$c: \text{Static linear base shear strength factor, } c = \frac{V_{\text{LinearStatic}}}{W} \quad (5)$$

$$\gamma: \text{Yield strength factor, } \gamma = \frac{F_y}{W} \quad (6)$$

$\eta$ : Maximum strength factor or strength factor,

$$\eta = \frac{F_{\max}}{W} \quad (7)$$

These parameters are available in Table 4 and for more comprehend discussion some of them have been shown by diagrams in Fig. 12.

It could be seen more ductility in MF models in all number of stories than EBF ones. The trend of ductility diagram for EBFs with long link-beam is different from other systems. The rate of ductility changes in EBF system with long link-beam rises by increasing the number of stories but in the other systems constant or decreasing patterns have been observed. The EBFs with short link-beam has much more ductility than the EBFs with long link-beam providing more capacity of energy absorbing and better nonlinear behavior.

Also, it could be seen that the EBFs with all number of stories could suffer more base shears than MFs. If we assess base shear and displacement diagrams simultaneously, it could be discovered that by the same displacement the EBF systems with short link could suffer more base shears which is because of more ductility and better nonlinear behavior of these systems in comparison with EBF systems with long link-beam illustrating the significance of nonlinear zone in displacement of EBF ( $e=0.5m$ ).

Parameter  $\eta$  is a useful parameter which facilitates finding out maximum base shear only by its application to weight of model and without performing time consuming nonlinear analysis. As we could see in Fig. 12, this parameter has the same trend for all systems and is more for EBFs than MFs.

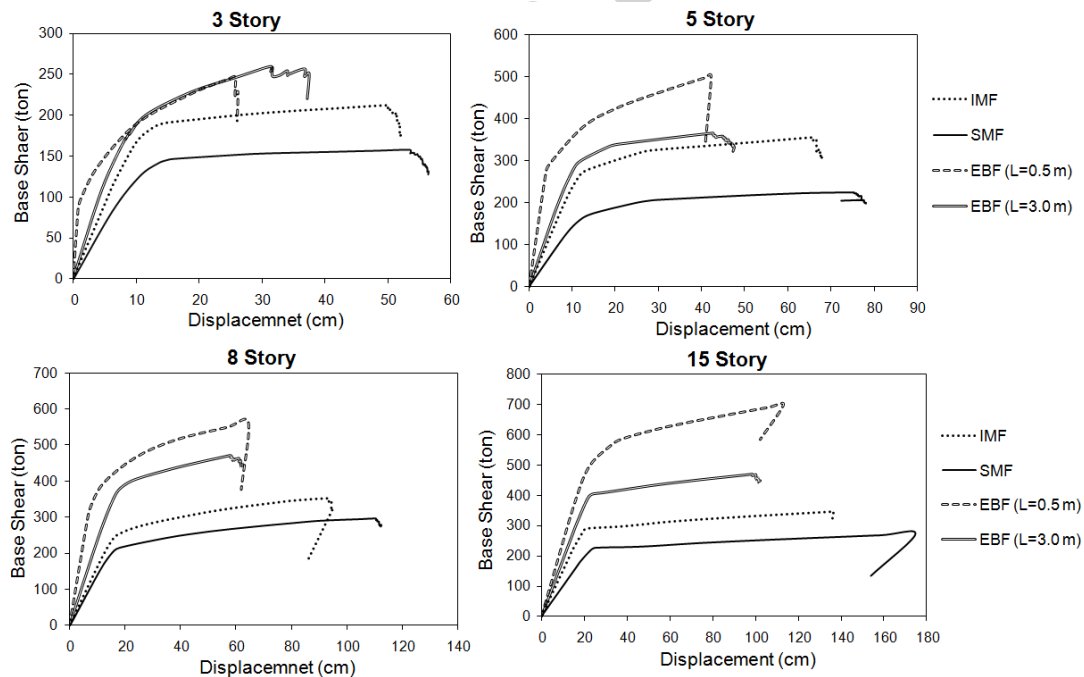


Fig.11. Pushover diagrams for models by different earthquake resisting system

Table 4. Nonlinear parameters

System No of Stories	Max Base Shear F <sub>max</sub> (ton)	Yield Base Shear F <sub>y</sub> (ton)	Max Displacement Δ <sub>max</sub> (cm)	Yield Displacement Δ <sub>y</sub> (ton)	μ	T (s)	V Lstatic (ton)	Weight (ton)	η F <sub>max</sub> /W	γ F <sub>y</sub> /W	c V Lstatic/W
IM-3	212.027	165.54	49.9	12.39	4.02	0.843	61.08	500.661	0.42	0.33	0.12
SMF-3	157.53	140.887	55.56	13.38	4.152	1.006	42.263	497.211765	0.32	0.28	0.09
EBF (e=0.5 m)-3	248.04	138.88	25.7	7.05	3.64	0.3438	47.119	376.952	0.66	0.37	0.13
EBF (e=3.0 m)-3	259.661	192.27	31.37	10.6	2.96	0.749	63.511	508.088	0.51	0.38	0.13
IM-5	356.2	267.988	65.94	12.28	5.37	0.914	81.581	867.882979	0.41	0.31	0.09
SMF-5	224.981	163.756	75.1	12.86	5.84	1.214	56.387	854.348485	0.26	0.19	0.07
EBF (e=0.5 m)-5	502.355	335.713	42.22	8.56	4.93	0.532	107.052	856.416	0.59	0.39	0.13
EBF (e=3.0 m)-5	365.655	309.04	42.72	13.78	3.1	0.86	109.372	874.976	0.42	0.35	0.13
IM-8	351.787	243.18	93.63	16.47	5.7	1.404	104.973	1399.64	0.25	0.17	0.08
SMF-8	296.41	215.29	110.5	17.84	6.194	1.38	74.089	1424.78846	0.21	0.15	0.05
EBF (e=0.5 m)-8	562.54	685.398	64.36	12.644	5.09	0.818	143.671	1408.53922	0.40	0.49	0.10
EBF (e=3.0 m)-8	472.01	368.58	58.08	17.035	3.41	1.179	144.89	1420.4902	0.33	0.26	0.10
IM-15	347.274	291.29	135.89	21.01	6.47	2.35	148.02	2741.11111	0.13	0.11	0.05
SMF-15	272.38	218.82	174.87	23.081	7.57	2.087	103.335	2719.34211	0.10	0.08	0.04
EBF (e=0.5 m)-15	698.93	487.92	113.243	21.694	5.22	1.45	203.732	2716.42667	0.26	0.18	0.08
EBF (e=3.0 m)-15	469.021	402.49	98.712	23.446	4.211	2.021	203.172	2708.96	0.17	0.15	0.08

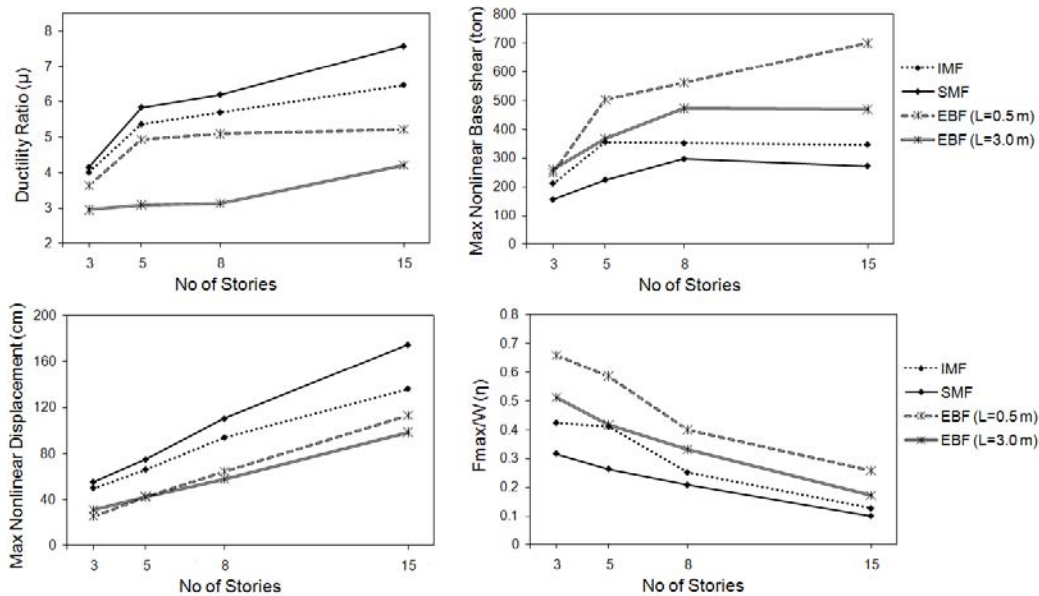


Fig.12. some nonlinear parameters for different systems with different number of stories

4.4. Evaluation of R (strength reduction factor) parameter

Behavior of a structure could be accessed through various approaches. If a structure behaves linear and exhausts inserted energy as an elastic system, its behavior is like diagram Fig. 13(a). If the design has been done considering all the hinges of a structure were formed simultaneously and all of them were fully elasto-plastic and no time gap assumed between the time of beginning nonlinear behavior in a specific point and entirely altering that point to hinge; then, the behavior of the model is like diagram Fig. 13(b) however, the actual behavior of a typical model is like diagram Fig. 13(c). We see in diagram (c) up to  $V_s$  the behavior is elastic, the difference between  $V_s$  and  $V_y$  is named strength reduction in view of over strength. Some codes utilize less base shear than  $V_s$  for design; but, they apply more coefficients for earthquake loads in load combinations. In the other word, they adjust design

in allowable stress level ( $V_w$ ). Iran's seismic code applied  $V_w$  and ASCE applied  $V_s$  for static linear analysis.

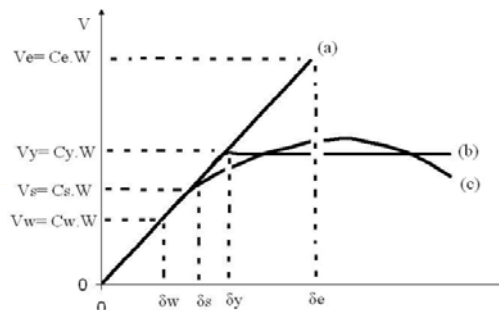


Fig.13. Different behavior of structures

Applied parameters could be defined as:

$R_{ductility}$  or  $R_d$  : Response factor of ductility

$$R_{ductility} = R_d = \frac{C_e}{C_y} \quad (8)$$

$\Omega_o$  or  $R_o$  : Response factor of over strength

$$\Omega_o = R_o = \frac{C_y}{C_s} \quad (9)$$

$R_{Allowable\ Stress}$  or  $R_{as}$  : Response factor of allowable stress level,

$$R_{Allowable\ Stress} = R_{as} = \frac{C_s}{C_w} \quad (10)$$

So we have

$R_w$  = Response factor of structure according to allowable stress level,

$$R_w = R_d \times R_o \times R_{as} \quad (11)$$

$R_s$  = Response factor of structure according to first hinge fabrication,

$$R_s = R_d \times R_o \quad (12)$$

$R_{ductility}$  Could be calculated from equality between the area under diagram (c) and diagram (a) for each model.  $R_{Allowable\ Stress}$  is usually considered 1.4 and  $R_o$  is calculated from the equation below:

$$R_o = R_{size} \times R_{\phi} \times R_{yield} \times R_{sh} \times R_{mech} \quad (13)$$

Where:

$R_{size}$ : consider the effects of model's size

$R_{\phi}$ : consider the effects of actual and nominal yielding

$R_{yield}$ : consider the effects of first and second yielding

$R_{sh}$ : consider the effects of strain hardening

$R_{mech}$ : consider the effects of mechanism and hinge generation.

We could gain these parameters from Table 5 [15].

Containing values of  $R_{as}$  and  $R_o$ , comparison between the R values from models, Iran's seismic code (UBC97) and ASCE was performed and mentioned in Table 6. It is realized that by increasing the building height the R values increases too. This is the disregarded fact in almost all codes that the R value changes by changing the height of buildings or by changing the period of structures.

If we calculate the mean value for  $R_s$  and  $R_w$ , we reach to Table 7. It is observed that the value of  $R_s$  for IMFs is larger than the R assumed in ASCE presenting better nonlinear behavior than what expected in this code for IMF systems. The  $R_s$  for SMF systems is approximately similar to R assumed in ASCE and  $R_s$  for EBF systems are smaller than the R assumed in ASCE code which means that the code overestimation of nonlinear behavior for EBFs. The  $R_w$ s got from analysis are more than the amounts of R considered in Iran's seismic code (similar to UBC97), which means of underestimation of this code for nonlinear properties for all of the systems.

Although, assumed R factors for IMF systems are less than EBF systems in ASCE code, the calculated R factors for IM and EBF systems are approximately equal implying approximately same nonlinear behavior of these systems; however, if we consider Fig. 12, better nonlinear behavior and more ductility were recognized for IMs than EBFs. Therefore, using only R factors for assessing nonlinear behavior could cause some confusing errors in deductions.

Table 5. Parameters used for calculation over strength reduction factor for steel structures [15]

System	Cat	Calculation of $R_o$						Proposed $R_o$
		$R_{size}$	$R_{\phi}$	$R_{yield}$	$R_{sh}$	$R_{mech}$	$R_o$	
Moment Resisting Frames	D	1.05	1.11	1.10	1.15	1.00	1.47	1.50
	MD	1.05	1.11	1.10	1.15	1.00	1.47	1.50
	LD	1.05	1.11	1.10	1.05	1.00	1.35	1.30
Concentrically Braced Frames	MD	1.05	1.11	1.10	1.05	1.10	1.48	1.50
	LD	1.05	1.11	1.10	1.05	1.00	1.35	1.30
Ecentrically Braced Frames	D	1.05	1.11	1.10	1.15	1.00	1.47	1.50
	LD	1.10	1.11	1.10	1.10	1.10	1.63	1.60
	LD	1.10	1.11	1.10	1.05	1.05	1.48	1.50
Conventional Constr.	-----	1.05	1.11	1.10	1.00	1.00	1.28	1.3

D-Ductile, MD- Moderately Ductile, LD-Limited Ductile

Table 6. The comparison of calculated R by the amounts in ASCE and Iran's seismic code2800

System No of Stories	Rd	Ro	Rs=Rd.Ro	R (ASCE)	Ras	Rw=Ras .Rs	R 2800
IM-3	3.71	1.47	5.45	4.50	1.40	7.64	7.00
SMF-3	4.71	1.47	6.92	8.00	1.40	9.69	10.00
EBF (e=0.5 m)-3	3.68	1.47	5.41	7.00	1.40	7.57	7.00
EBF (e=3.0 m)-3	3.48	1.47	5.12	7.00	1.40	7.16	7.00
IM-5	4.26	1.47	6.26	4.50	1.40	8.77	7.00
SMF-5	5.77	1.47	8.48	8.00	1.40	11.87	10.00
EBF (e=0.5 m)-5	3.77	1.47	5.54	7.00	1.40	7.76	7.00
EBF (e=3.0 m)-5	4.26	1.47	6.26	7.00	1.40	8.77	7.00
IM-8	4.33	1.47	6.37	4.50	1.40	8.91	7.00
SMF-8	5.46	1.47	8.03	8.00	1.40	11.24	10.00
EBF (e=0.5 m)-8	4.25	1.47	6.25	7.00	1.40	8.75	7.00
EBF (e=3.0 m)-8	4.05	1.47	5.95	7.00	1.40	8.33	7.00
IM-15	4.48	1.47	6.59	4.50	1.40	9.22	7.00
SMF-15	6.12	1.47	9.00	8.00	1.40	12.59	10.00
EBF (e=0.5 m)-15	4.81	1.47	7.07	7.00	1.40	9.90	7.00
EBF (e=3.0 m)-15	4.21	1.47	6.19	7.00	1.40	8.66	7.00

Table 7. comparison between ( $R_s$  and R (ASCE)) as well as ( $R_w$  and R 2800) (Iran's Seismic Code)

System No of Stories	Rs	R (ASCE)	Rw	R 2800
IM	6.17	4.50	8.63	7.00
SMF	8.11	8.00	11.35	10.00
EBF (e=0.5 m)	6.07	7.00	8.49	7.00
EBF (e=3.0 m)	5.88	7.00	8.23	7.00

#### 4.5. Evaluation of nonlinear parameters from nonlinear static and dynamic analysis

One simple method for assessing nonlinear parameters under a specific record is considering lateral story shears by nonlinear dynamic analysis under that record as the input distribution for nonlinear static analysis. It means in our research as there are 12 records, 12 pushover analyses should be done for each model or  $12 \times 16 = 192$  pushover analyses for all of the models. Then the mean of results should be calculated for two groups of records, near and far-field records. In this research, the mean of lateral shears under nonlinear dynamic analysis for near and far-field earthquakes have been employed as the input shear distribution for pushover analysis of each model. By this technique, the number of pushover analysis reduced to 2 for each model, one for near-field and one for far-field earthquakes, or 32 analyses for all of the models.

As we could see in Fig. 14, for all of the systems the ductility demands under near-field earthquakes are much more than ductility demands under far-field ones and also more than the ductility capacity of the system calculated from static nonlinear analysis. Therefore, under these records collapse takes place before reaching hinges to ultimate level of their nonlinear performance. Also, it could be recognized that in MFs, ductility demands from far-field records are less than their capacities, but in EBFs the demands under far-field records are a little more than capacities except in EBFs with short link-beams in low rise models.

The patterns of ductility demand against far-field and near-field records are different; therefore, we could not use amplification factor to attain ductility demand from far-field records rather than near-field ones and we must do analysis for near-field earthquakes individually.



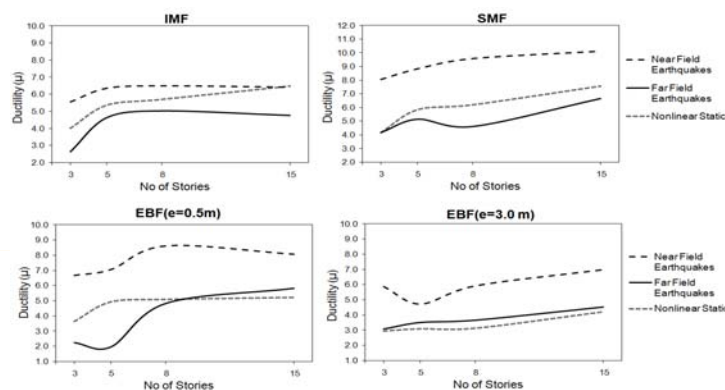


Fig. 14. Ductility for different systems under near and far-field earthquakes and static nonlinear analysis

#### 4.6. Distribution of ductility demands in height of structures and proposing practical method for its calculation

Ductility demand and capacity distribution in height of structure is one of the parameters that influence structural nonlinear behaviors. For obtaining each story's ductility, one frequently used method is to perform nonlinear static analysis by considering the displacement of that story as a control point which omits most of the upper stories effects and contributes some errors in results.

The other method that was used and proposed in detail in this research is considering rotation in each hinge and defining level of ductility for each hinge. Then according to consisted hinges, story ductility could be obtained by calculation of hinges average ductilities. For instance, in Table 8, adjusted table for reaching the distribution of ductility in height for 5-story IMF system under nonlinear static analysis is mentioned. We could see the number of hinges in each ductility group for each story and the amount of assumed ductility for each of the ductility groups extracted from FEMA273 [14]. For better understanding of Table 8, some necessary information of FEMA273 [14] was mentioned in Fig. 15. Tables of ductility distribution were generated for all of the models under near-field and far-field earthquakes and also static nonlinear analysis similar to Table 8. For simplifying the comparison diagrams of Figs 16 to 18 were prepared.

It could be noticed that by increasing the height of structures and increasing period of systems, maximum ductility demand occurs in higher stories. This fact has been intensely observed in buildings with more number of stories and under near-field earthquakes. The patterns of ductility distribution under near-field earthquakes are more similar to the pattern of ductility capacity distribution; however, the pattern of ductility distribution under far-field records is different with both of those patterns. But, the amounts of ductility demands under far-field records are closer to the amounts of ductility capacity than near-field records. Having larger ductility demand than ductility capacity indicates that the structure comes to collapse before it can reach to its ultimate nonlinear performance level. So, structures under near-field records encounter leakage of ductility especially in the middle stories.

The shape of ductility diagrams under near and far-field earthquakes are different, consequently, for getting the ductility demands under near-field records we could not use a modification factor to the ductility demands from far-field earthquakes and we should do

analysis for near-field earthquakes individually.

Table 8. Ductility's distribution in height for 5-story IMF under nonlinear static analysis

Story's Number	Step 9								Story's Ductility	Percent of Ductility Demand for each Story
	A-B	B-IO	IO-LS	LS-CP	CP-C	C-D	D-E	>E		
5	0	32							48	8.82
4		16	16						80	14.71
3				17	1	3	11		164	30.15
2			5	26		1			140	25.74
1			32						112	20.59
0	0	0	0	0	0	0	0	0	0	0.00

Structural Performance Levels: IO: Immediate Occupancy; LS: Life Safety; CP: Collapse Prevention

Sum= 544

Component/Action	Modeling Parameters			Acceptance Criteria					
	Plastic Rotation Angle, Radians	Residual Strength Ratio	c	Plastic Rotation Angle, Radians					
				Primary		Secondary			
	a	b		IO	LS	CP	LS	CP	
Beams—flexure									
a. $\frac{b_f}{2t_f} \leq \frac{52}{\sqrt{F_{ye}}}$ and $\frac{h}{t_w} \leq \frac{418}{\sqrt{F_{ye}}}$	90 <sub>y</sub>	110 <sub>y</sub>	0.6	10 <sub>y</sub>	60 <sub>y</sub>	80 <sub>y</sub>	90 <sub>y</sub>	110 <sub>y</sub>	

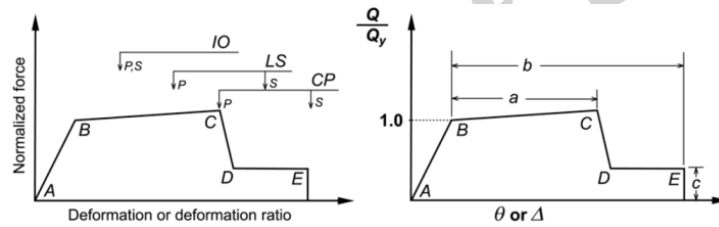


Fig.15. some complementary information about table 4 from FEMA 273

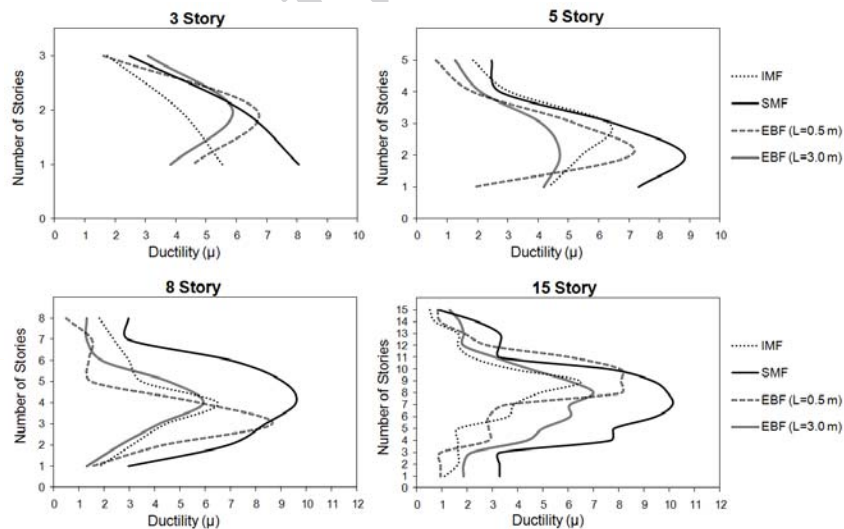


Fig.16. Distribution of ductility demands under near-field records

It should be mentioned that since the period of structures are variable in addition to the

kind of seismic resisting systems, the comparison might have some errors, for accurate comparison it is more convenient to use different systems with same period; however, the aim of this research is evaluation of the actual structural systems designed consistent with common codes and specifications; then, both period and kind of seismic resisting system of models are variable.

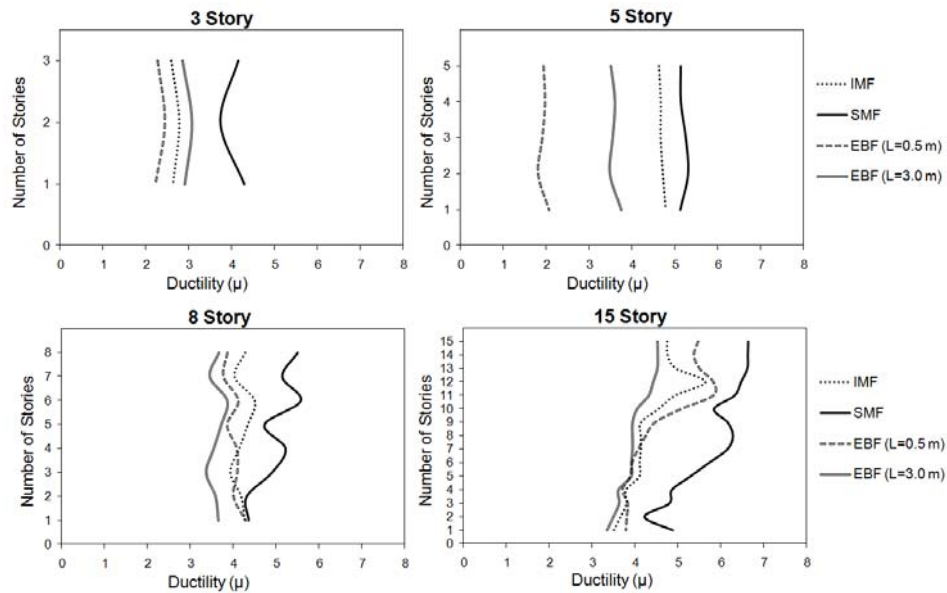


Fig.17. Distribution of ductility demands under far-field records

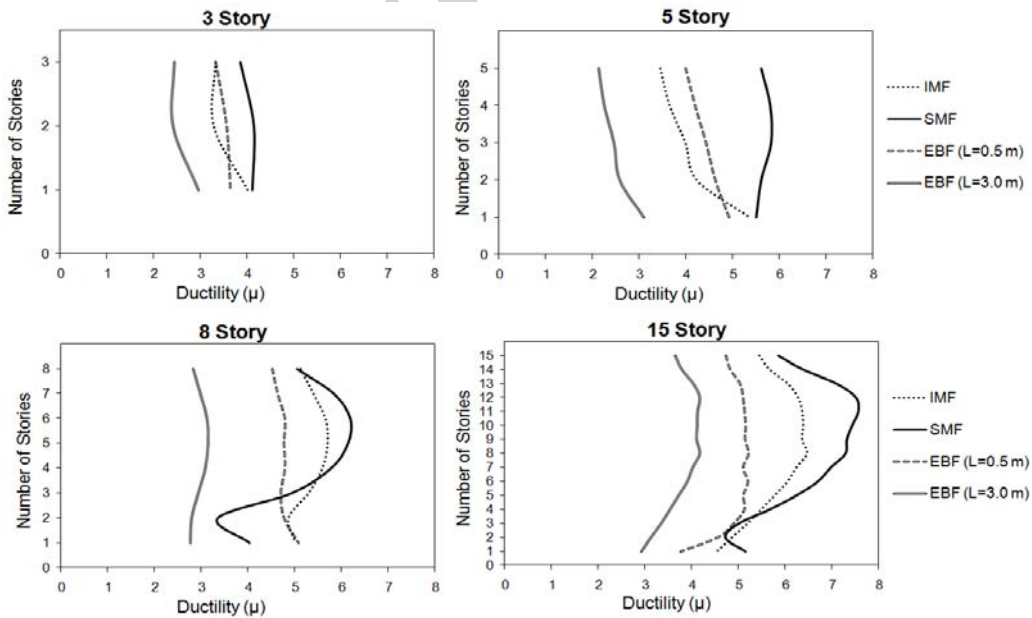


Fig.18. Distribution of ductility capacity from nonlinear static analysis

## 5. CONCLUSIONS

A comprehensive evaluation and comparison of two frequently used structural systems have been done and a practical method for obtaining the demand distributions is proposed in this research employing common software for analyzing and design. Some conclusions of this research are mentioned below:

- Standard deviation of results under different records from linear analysis is remarkably less than these values from nonlinear analysis for both MF and EBF systems. Also, standard deviation of results under near-field records are a lot more than far-field ones.

- There is less dispersion in behavior of EBF than MF systems showing more accuracy in application of mean values for EBF systems than MF systems.

- The least lateral story shears have been observed in SMF systems and the most in EBF systems with short link-beams from nonlinear dynamic analysis.

- The amounts of lateral story shears for different systems are very close to each other under far-field records, in spite of their considerable differences under near-field ones.

- The negative or inverse story shears have not been observed in shear distribution diagrams of EBF systems with short link-beams under near-field earthquakes, whereas for the other systems negative shears usually exist in some stories below the roof story.

- It could be seen for all of the systems under both near-field and far-field earthquakes by increasing number of stories, maximum story shear moves to the lower height ratios. This fact is more intense in SMFs than the other systems.

- The mode propagation effects under near-field records are much more participated in distribution of shears and displacements than far-field ones. Mode participation could be noticed in moment frame systems much more than EBF systems and it is one of the important motivations for transmission of maximum story shear to lower height ratios and occurrence of negative shears.

- For all of the systems, shears from linear dynamic analysis under far-field records are less than shears from linear static analysis and shears from near-field records are approximately equal or more than linear static results particularly in the middle stories. Similarities between results from linear dynamic analysis under near-field earthquakes with the linear static results in MF systems are more than EBF systems.

- The EBFs with short link-beams are able to suffer more lateral forces than EBFs with long link-beams in nonlinear analysis, but in linear analysis the distributions and amounts of lateral forces in both systems are close to each other. It shows that the nonlinear capacity of EBFs with long link-beams is less than the capacity of this system with short link-beams and the most shear capacity of EBFs with short link-beams is in nonlinear region.

- It could be inferred from nonlinear dynamic analysis that in EBF ( $e=3.0m$ ) with three and five stories lateral displacements are more than EBF ( $e=0.5m$ ). But by rising the number of stories and extending nonlinear behavior of models, lateral displacements in EBF ( $e=0.5m$ ) become more than EBF ( $e=3.0m$ ).

- More ductility could be seen in MF systems than EBF systems in models with all number of stories. The trend of ductility diagram for EBFs with long link-beam is different from other systems. The rate of ductility changes in EBF system with long link-beam rises by increasing number of stories but it become constant or decrease in the other systems.

- By the same displacement, the EBF systems with short link-beams could suffer more

base shears compared to EBF systems with long link-beam that is because of more ductility and nonlinear behavior of these systems.

- The distribution of parameter  $\eta$ , the maximum base shear divided by the weight of model, corresponding to the number of stories has the same trend for all of the systems and its value is more for EBF systems than MF systems.

- By increasing the buildings height, the R factor (strength reduction factor) increases too. Whereas changing the R values corresponding to height or period of structures is the disregarded fact in design codes.

- It is observed that the R values for IMFs are larger than the R assumed in ASCE. This means that the nonlinear behavior of these systems is better than what expected in this code. The R for SMF systems is approximately similar to R assumed in ASCE and R values for EBF systems are smaller than the R assumed in ASCE code which means the code overestimation of nonlinear behavior for EBFs. The R values got from analysis are more than R values considered in Iran's seismic code (similar to UBC97), which means underestimation of these codes about nonlinear properties for all of the systems.

- Although the assumed R factors for IMFs are less than EBFs in ASCE code, the calculated R values for IM and EBF systems are approximately equivalent presenting almost same nonlinear behavior of these systems.

- For all systems, the ductility demands under near-field earthquakes are much more than ductility demands under far-field ones and ductility capacities; therefore, collapse was occurred before reaching hinges to ultimate level of their nonlinear performance under near-field records.

- It could be recognized that MF's ductility demands from far-field records are less than their capacities, but EBF's ductility demands under far-field records are a little more than their capacities except in EBFs with short link-beams in low rise models.

- The patterns of ductility demand distribution against far-field and near-field records are different; therefore, we could not use amplification factor to attain ductility demand from far-field records rather than near-field ones and we must do analysis for near-field earthquakes individually.

- By increasing the height of structure and period of system, the maximum ductility demand occurs in higher stories. This fact has been seen more in buildings with more number of stories and under near-field earthquakes.

- The patterns of ductility demand distribution under near-field earthquakes are more similar to the pattern of distribution of ductility capacity; however, the pattern of ductility demand distribution under far-field records is different with both of those patterns. But, the amounts of ductility demands under far-field records are closer to ductility capacities than ductility demands under near-field records.

## REFERENCES

1. Naeim F. *The Seismic Design Handbook*, Kluwer Academic Publishers, 2nd edition, 2001.
2. *Seismic Design Recommendations SEAOC Blue Book*, Seismology Committee of the Structural Engineers Association of California, 1996.

3. Combescure D, Queval JC, Sollogoub P, Bonnici D, Labbe P. Effect of Near-Field Earthquake on a R/C Bearing Wall Structure Experimental and Numerical Studies, *11th European Conference on Earthquake Engineering, Balkema, Rotterdam*, Bookfield, 1998, pp. 189-99.
4. Iwan WD. Near-Field Consideration in Specification of Seismic Design Motions for Structures, *10th European Conference on Earthquake Engineering, Balkema, Rotterdam*, 1995, pp. 257-67.
5. Malhotra PK. Response of buildings to near-field pulse like ground motion, *Earthquake Engineering*, **28**(1999) 1309-26.
6. UBC97, Structural Engineering Design Provisions, *International Conference of Building Officials Uniform Building Code*, California, USA, **2**(1997).
7. Somerville P, Smith N, Punyamurthula S, Sun J. *Development of Ground Motion Time Histories for Phase 2 of the FEMA/SAC Project*, Report NO. SAC/BD-97-04, Available from <http://www.sacsteel.org>, 1997.
8. SAC Database Center, (Structural Engineers Association of California (SEA), Applied Technology Council (ATC), California Universities for Engineering (CUREe)), <http://www.sacsteel.org>.
9. Iran's Building and House Research Center, <http://www.bhr.gov.ir>.
10. Pacific Earthquake Engineering Research Center (PEER), PEER Strong Motion Database, <http://peer.berkeley.edu/smcat>.
11. 2800 Standard, Iran's Seismic Provisions for design of buildings, *Building and House Research Center, Iran*, **3**(2005).
12. *Iran's Provisions for Design and Construct of Structural Steel Buildings*, The Ministry of Housing & Urban Development, Iran, 2005.
13. AISC, *Manual of Steel Construction*, American Institute of Steel Construction, Chicago, U.S.A, 2005.
14. FEMA, (Report No. FEMA 273), *Building Seismic Safety Council for the Federal Emergency Management Agency*, NEHRP Guideline for Seismic Rehabilitation of Buildings, Washington DC, USA, 1997.
15. ASCE, VA: (ASCE 7-05), *Minimum Design Loads for Buildings and Other Structures*, American Society of Civil Engineers, Reston, USA, 2002.